LONG DRIFT TECHNIQUES FOR CALORIMETERS

L.E. PRICE
Argonne National Laboratory
Argonne, IL 60439

There are several advantages that can be expected from the use of long drift chambers as the sensitive element in gas-sampling calorimeters in place of closely-spaced proportional cells. These advantages include a sharply reduced number of wires to read out, a detailed image of each shower, and the possibility of processing the detailed signals to improve the energy resolution. We report here on the development of the thin-gap chambers, up to 50 cm long, that are needed for calorimetry, on the results of tests of a working drift-collection calorimeter, and on the design of a calorimeter for use in a solenoidal detector at the SLAC Linac Collider. Operation in a magnetic field is discussed.

Introduction

Long drift chambers have gained a prominent position among detectors for High Energy Physics (viz. ISIS, TPC, JADE) because of the large quantity of information they produce about an individual event. Typically a complete "image" of the event is formed with the spatial coordinates. Equally important advantages can be expected from the application of the long drifting technique to calorimeters, i.e., the use of long (but now thin) drift chambers as the sensitive element between radiator plates in a gas-sampling calorimeter[1].

1. A time history of each signal element--wire or cathode pad--can be read out to provide a complete image of the cascade.

2. Processing of the detailed map of ionization --either later in a computer or immediately in hardware--can be used to improve the energy resolution and regain some of the degradation of resolution that is normally associated with gas as a sampling medium.

3. Readout in time buckets produces a high degree of segmentation while keeping the number of fragile wires and the number of readout channels modest.

4. Along with the number of readout channels, the cost is modest.

On the negative side, the long readout time will preclude the use of drifting calorimeters in very high rate environments.

Development of Long Drift Chambers

The new problems that must be overcome for the use of long drift chambers in calorimeters can be discussed in connection with Figure 1, which shows a sketch of the 50 cm drift chambers we are developing for a nuclear decay search[2]. The drift electric field is produced by a pattern of conducting strips on an insulating substrate which are connected to an external resistor chain. At the end of the drift region, the ionization electrons are amplified by an anode wire surrounded on three sides by cathode, which can be segmented and readout as pads to give the coordinate along the wire. The chambers must normally be kept thin so the density of the calorimeter remains high. Thus the drifting electrons are always near the walls and in danger of drifting into the walls and being lost.

Two effects in particular produce the loss of electrons on the walls. The effects and our solutions to them, are as follows:

1. With a discrete drift electrode, conductors outside of the drift chamber can affect the field inside. In particular, with the applied potentials as shown in Figure 1, the grounded radiator plates outside the chamber distort the field in such a way that most drifting electrons which start from the maximum drift distance drift to the walls instead of to the anode wire. Calculated equipotential lines are shown in Figs. 2a (no grounded plates) and 2b (with grounded plates). We have overcome this distortion of the drift field by covering the drift electrode--both conducting strips and dielectric--with resistive ink of surface resistivity approximately 10^{10} ohm/square . The resistive ink continues the resistive divider chain to every point inside the chamber, so that the potential is determined at every point on the boundary and hence the field inside the chamber is completely determined. The resulting calculated equipotentials are shown in Fig. 2c.

2. Even when the electric field inside the chamber does not direct the drift electrons into the walls, some electrons will be lost by transverse diffusion into the walls[4]. This loss is an inescapable consequence of drifting in extreme aspect ratio geometries. The system we have developed minimizes this effect, however by a) using a gas with a low electron temperature[5] such as 90Ar, $10CO_2$; and b) applying a focussing drift electric field, i.e. one with a component at the walls that will drift electrons toward the center of the chamber. A constant angle of the field at the walls is provided by an exponentially distributed potential[4].

$$\phi = \phi_0 + a \exp(-bz) \cos(by),$$

where the origin of coordinates is at the anode wire,

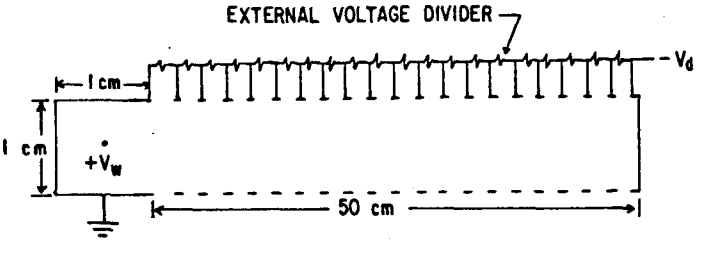

Fig. 1. Cross-section of prototype chamber with 50 cm drift length. The drift field is shaped by the conducting strips (printed circuit lines) connected to an external resistor chain as shown and also by a continuous film of resistive ink (not shown) that interpolates the potential between conducting strips. Top and bottom conductors are connected to the same resistor chain. Note that the vertical and horizontal scales are different.

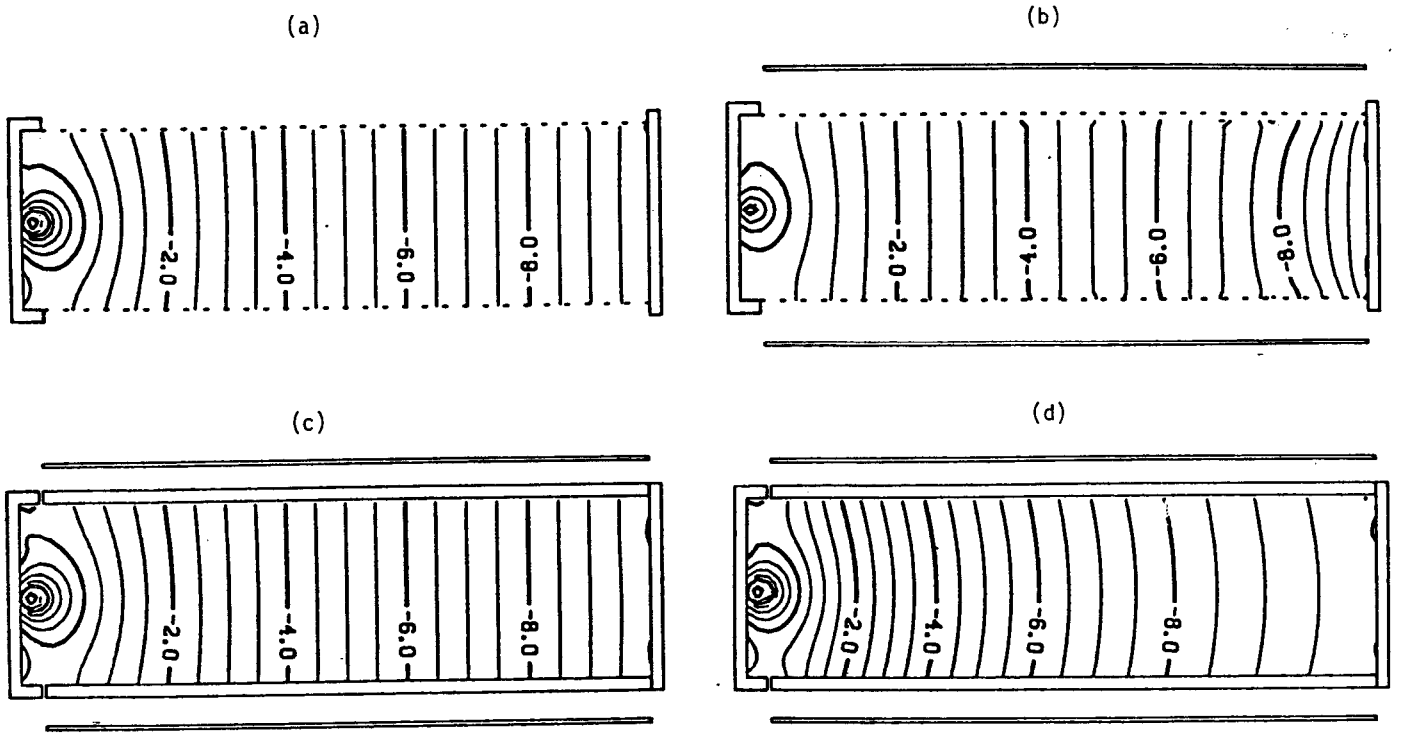

Fig. 2. Equipotential plots in the 50 cm chamber for a) linear resistor chain with discrete electrodes; b) same with nearby grounded plates; c) linear resistor chain with continuous electrode (resistive ink), showing no effect from grounded plate; and d) exponential resistor chain with continuous electrode. The equipotentials are labeled in kilovolts.

the z axis is parallel to the drift direction, and the y axis is perpendicular to the anode wire. Since diffusion is related to random thermal processes, the focussing field does not completely eliminate losses of electrons, but can substantially reduce them. Equipotentials produced by an exponential resistor chain in a chamber with resistive ink on the walls, are shown in Fig. 2d.

The drifting performance of a chamber built along the lines described above is shown in Fig. 3. The gas used was 90Ar, $10Co_2$ with a total applied drift potential of 10kV. With a linear resistor chain, the attenuation after 50 cm drift is 30%--exactly what is predicted from diffusion alone. Only 12% attenuation is found with the exponential--or focussing--resistor chain, where the focussing parameter b was 0.03/cm. Again, this is consistent with what is expected from diffusion.

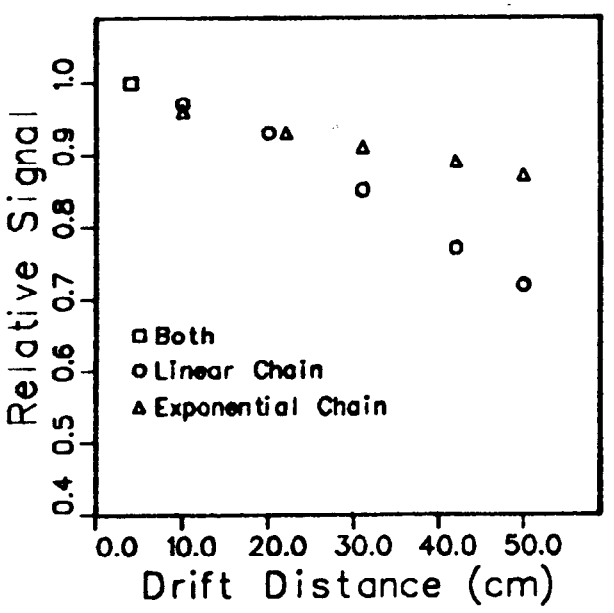

Fig. 3. Signal on sense wire as a function of drift distance for linear and exponential resistor chains. Measured signals have been corrected for attenuation from oxygen contamination and normalized to those outlined with 4 cm drift distance. All measurements are for V_d = 10 kV.

Electromagnetic Calorimeters

An electromagnetic calorimeter has been built and tested using long drift gaps. Although the aspect ratio for the drift gaps is similar to the chambers discussed above, the dimensions are smaller: drift gaps as small 2.4 mm were used for drift distances up to 76 mm. As shown in Fig. 4, the calorimeter was built in a single gas volume, with the electrons drifting to a PWC plane at one end of the radiator plates. Drifting performance with non-showering particle is shown in Fig. 5: the attenuation is 12% in a 2.4 mm gap after 76 mm drift, with an applied field of 350 v/cm in 90Ar, $10CH_4$ gas. With showering particles, the energy resolution of the calorimeter has been measured. As shown in Fig. 6, with $1X_0$ sampling, the resolution corrected for variations

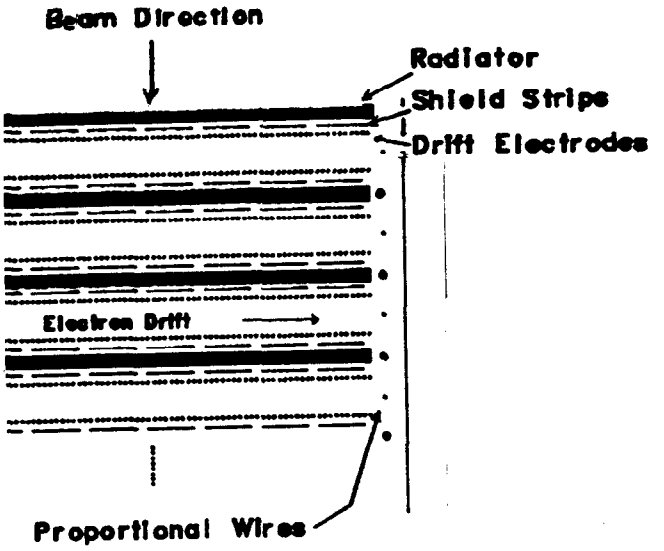

Fig. 4. Sketch of drift-collection electromagnetic calorimeter used in test beam. The drift region is 76 mm long and gaps as small as 2.4 mm were used. The lead raitator plates are 1 radiation length thick.

in the wire gain is $0.23/\sqrt{E}$. Fig. 7 shows the response of the calorimeter as a function of energy which is seen to be quite linear.

We have shown that the performance of the calorimeter is not degraded by the use of long drift gaps as sampling elements. Can the resolution be improved by processing the drifting signals? In Fig. 8, we show the results from the EGS Monte Carlo program of processing the signal in the following way:

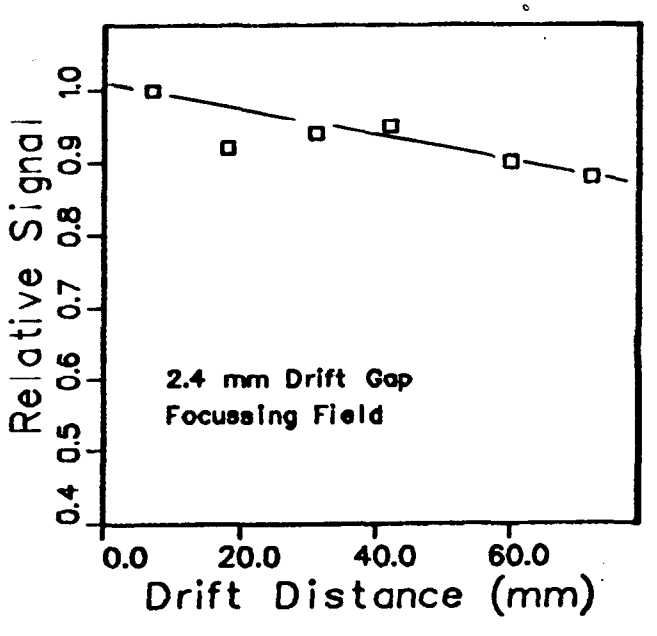

Fig. 5. Attenuation of drifting signals from non-showering signals in calorimeter with 2.4 mm drift gap width. See text for operating conditions.

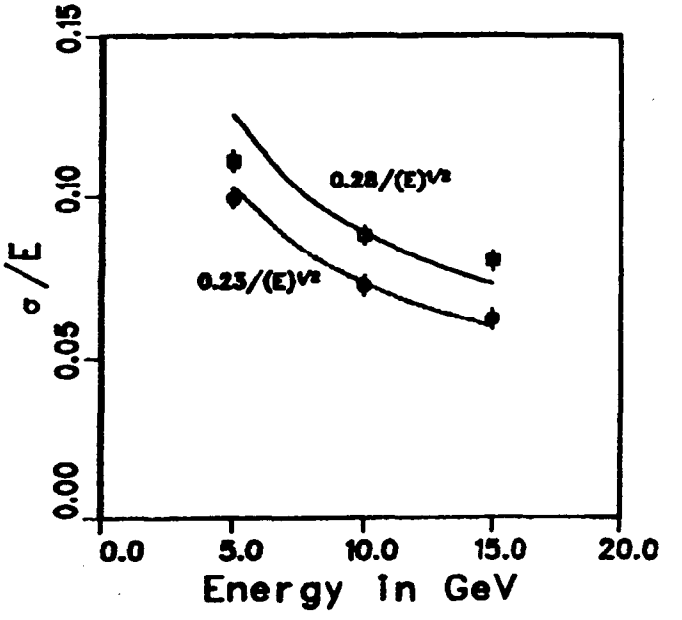

Fig. 6. Energy resolution for positrons in drift collection calorimeter at three energies with $1X_0$ sampling. After correcting for variations in the wire gain, the resolution is $0.23/\sqrt{E}$.

a) The signal is digitized in 1 mm bins along the drift direction.

b) Three longitudinal samples are used, with thicknesses $4X_0$, $6X_0$, and $10X_0$.

c) Outside a central core whose width in the

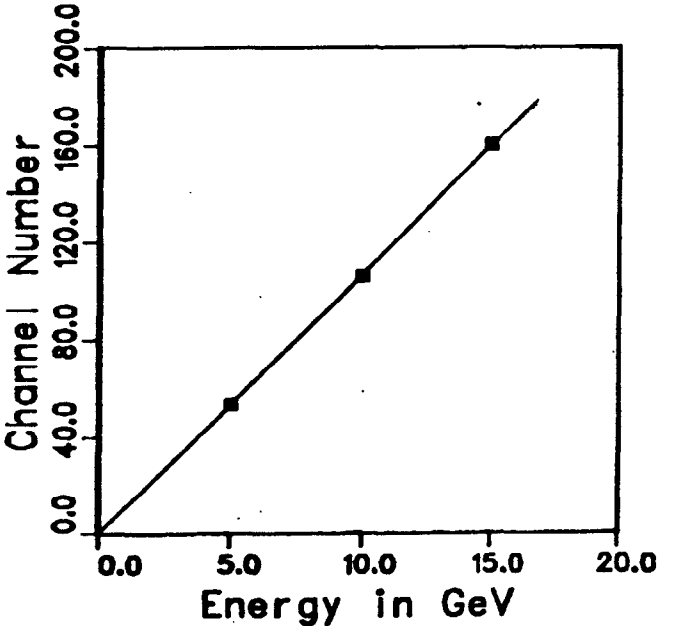

Fig. 7. Response of electromagnetic calorimeter as function of positron energy. No saturation is seen.

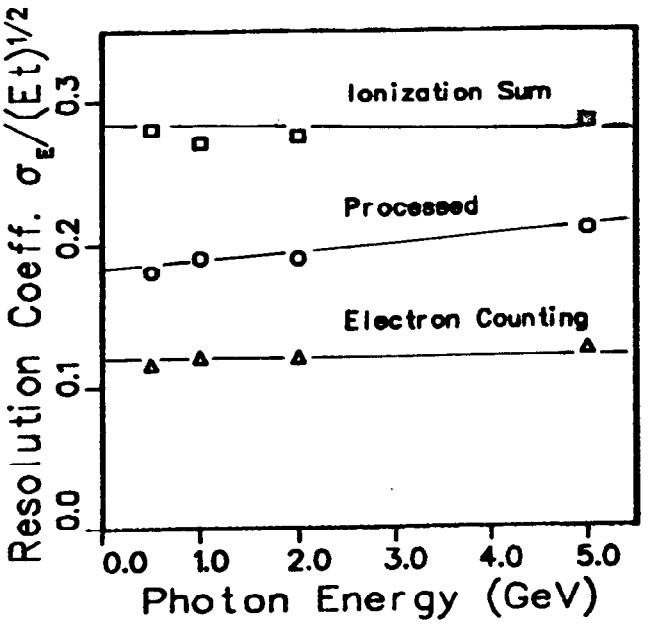

Fig. 8. Improvement of energy resolution by processing results of EGS Monte Carlo simulation as described in text. Up to 5 GeV, the result is a resolution about midway between ideal electron counting and simply summing the total ionization signal.

drift direction varies from ± 2 mm at 0.5 GeV to ± 6 mm at 5 GeV, any 1 mm bin whose signal is at least three times the single-electron average has that signal replaced by the single-electron average.

As seen in Fig. 8, the coefficient $\sigma_E/\sqrt{E_\ell}$ is improved from 0.28 to an average of 0.20 in the energy range from 0.5 to 5 GeV. The slow growth of the coefficient with increasing energy is related to the increasing width of the core region excluded from the processing.

Calorimeters for the SLC

A system of hadronic and electromagnetic calorimeters has been designed for use in a solenoidal magnetic detector at the proposed SLAC Linac Collider (SLC)[6]. The very low repetition rate of the SLC allows maximum use of drifting and of hardware processing before readout to a computer. The proposed calorimeter is shown in Fig. 9. It is arranged in a projective -geometry, with the electromagnetic calorimeter inside the coil and the hadronic calorimeter outside the coil. Readout is only from cathode pads in the readout gaps (which are conical). The longitudinal and azimuthal segmentation of the readout is determined by the shapes of the chathode pads. A list of parameters of the SLC calorimeter is given in Table I. The whole calorimeter including electromagnetic and hadronic sections in the barrel and endcap regions is read out with less than 25,000 electronic channels and gives segmentation of 1.5 mrad x 25 mrad.

Effect of Magnetic Fields

The calorimeter shown here has an electromagnetic part inside a solenoid magnet coil and therefore in the full mangetic field of the detector. The hadronic portion of the calorimeter is partly outside the coil, where it is subjected to smaller, but less predicably oriented magnetic fields. Can drift-collection calorimeters coexist with real magnetic fields?

Two directions of drift are used: axial drift between cylindrical plates in the barrel region; and radial drift between plates perpendicular to the magnet axis in the endcap region. The solenoidal field in which the drifting takes place is primarily axial, with a smaller radial component. In addition, there will be small azimuthal components arising from lack of cylindrical symmetry in the coil and flux return iron. The motion of drifting electrons is governed by the Lorentz force $F = e(E + v \times B)$, where v is the instantaneous velocity. Although the actual motion of the electrons is discontinuous, punctuated by frequent collisions with gas molecules, an adequate approximation is obtained by assuming a constant velocity $\langle v \rangle$ in the direction

$$(E + \langle v \rangle \times B). \qquad (1)$$

With this approximation, we can now discuss drifting in the barrel and endcap portions of the calorimeter. In the barrel, the large axial component of the magnetic field is not troublesome, as the electrons drift along it. Further, radial fields produce an azimuthal component of drift, which is still acceptable in a cylindrical drift gap. It can be largely eliminated by pitching the drift electric field so that $(E + \langle v \rangle \times B)$ is still axial. If the compensation is not exact, the result will be an azimuthal distortion of position at the readout wires which can be corrected for. Thus only the azimuthal component of magnetic field--which produces radial components of drift velocity and hence tends to lose drifting electrons on the plates--are damaging, and they can be kept small by proper design of the magnet.

In the endcap portion of the calorimeter, the radial component of B is along the direction of drift, while the main axial component produces an azimuthal component of drift velocity, which as above is tolerable and largely correctable by the direction of the electric field. Here again, it is the azimuthal magnetic field which produced drift into the plates, now with an axial motion.

We can use the approximate direction of equation (1) to calculate a limit on the azimuthal magnetic field. The parameters shown are such that half of the drifting charge will be lost if the angle of drift toward the plates is 0.005 radians. We equate this angle to $\langle v \rangle B\phi / E$, where $B\phi$ is the azimuthal component of B. If we take typical values of $\langle v \rangle = 1 \times 10^4$ m/sec and $E = 2 \times 10^5$ v/m (e.g. in 90 Ar, 10 CO_2) we find B = 0.01 Tesla = 100 gauss. In an axial field of, say, 5 kg this should be attainable. This analysis of drift directions agrees within about 25% with measured drift angles in magnetic fields. The disagreement with measurements, and indeed with a fuller analysis--are such that our calculations from (1) overestimate the effect of azimuthal fields.

The situation is improved by the use of focussing electric fields. In this case, the electric field at the plates always has a component toward the center of the drift gap, which tends to lessen the effect of azimuthal magnetic fields and of diffusion in the gas. In this case, the tolerable $B\phi$ can realistically be 300 gauss.

Electrodeless Drift Planes

A Manchester group has developed drift chambers that have no drift electrodes, but charge internal

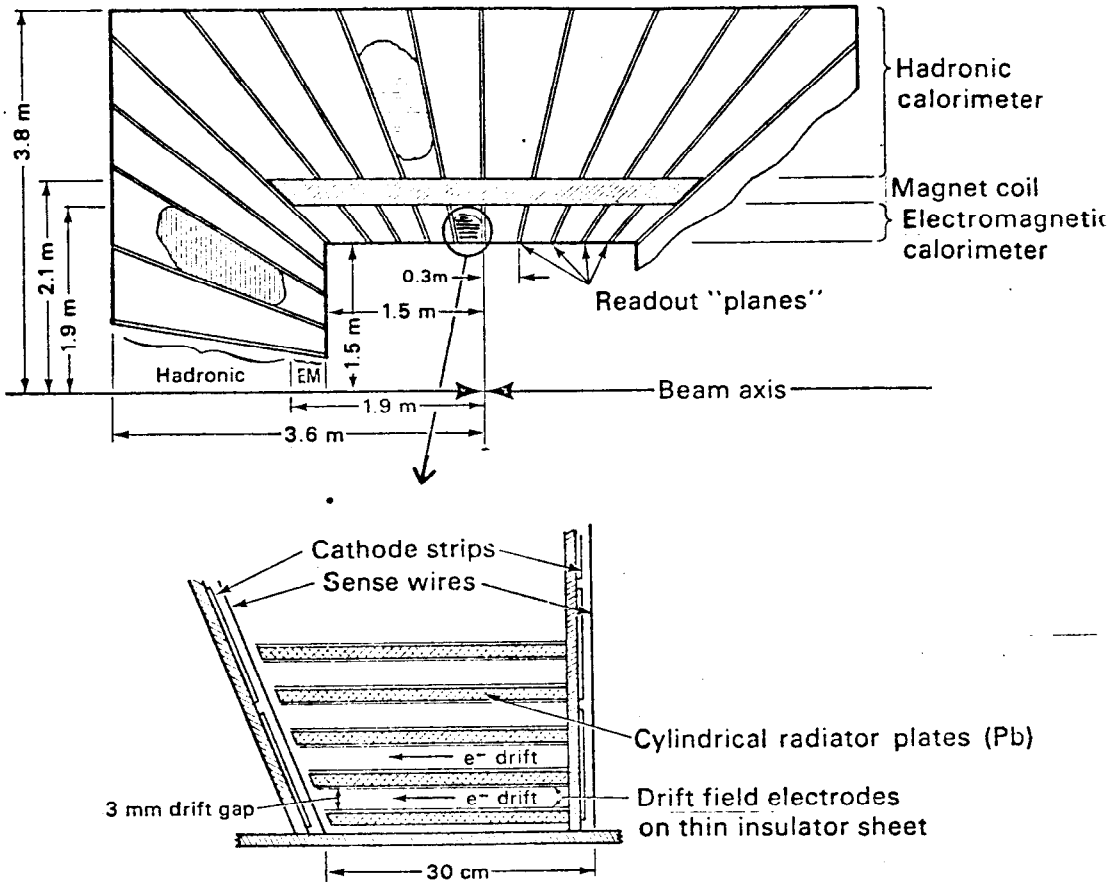

Fig. 9. Application of drift-collection calorimetry to a solenoidal detector for the SLC.

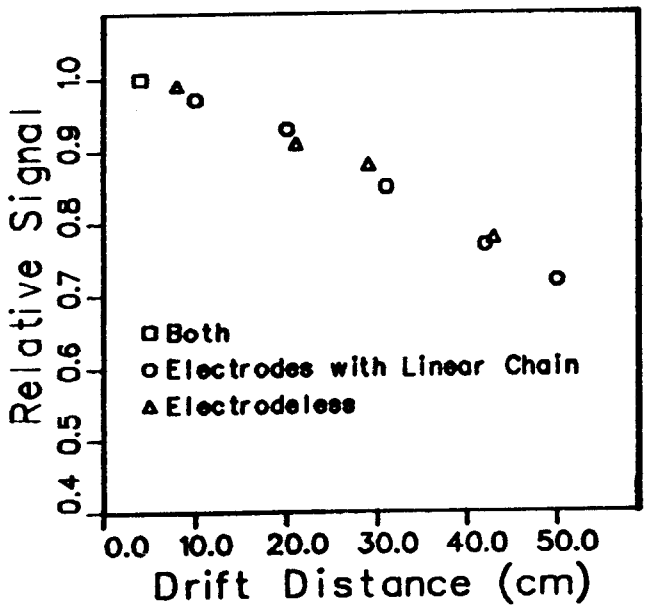

Fig. 10. Attenuation of drifting signals in electrodeless chamber with same dimensions as chamber in Fig. 1. See text for operating conditions.

dielectric surfaces to produce a drift field parallel to the walls[7]. Potentials are applied so that the outside surface of the chamber, which is conducting, is at the most negative potential. Positive ions, from avalanches at the wire, deposit themselves on the dielectric surfaces until field lines from the anode wire no longer intersect the wall but go all the way to the far end of the chamber, where there is a cathode inside the chamber. If such chambers are practical, the construction of a drift-collection calorimeter will be considerably simplified.

We have built an electrodeless drift chamber with the geometry of Fig. 1; we retained the local cathode on three sides of the anode wire as shown in Fig. 1 so that the wire gain could be controlled independently of the drift field. The chamber was operated similarly to the Nucleon Decay 50 cm chambers so that a good comparison could be made. The gas used was again 90Ar, 10 CO_2 with a drift field of 140 v/cm and the voltage between the anode and the local cathode was set to 1.7 kV. Drifting performance of this electrodeless chamber, after 24 hours charging with cosmic rays, is shown in Fig. 10. It is seen to be very similar to the attenuation obtained with electrodes and resistive ink using the linear resistor chain (Fig. 3). Further charging, however, over a period of 10 days, produced a deterioration of the drift performance. Our initial interpretation of this effect is that the charging of the dielectric surfaces continued beyond the optimum point by diffusion of the positive ions into the walls. If this is true, it may be difficult to achieve long-term stable behavior of these chambers. We are continuing to investigate these problems.

On the positive side, we note that the automatic charging of these chambers to the optimum field may make possible chambers that curve around a beam pipe or target . It may even be possible to make chambers that automatically compensate for magnetic fields that would bend drifting electrons into the walls. With magnetic fields, however, the charging will have to be done by electrons because the positive ions move with much lower velocities and therefore have less effect from the magnetic field.

Summary

We have shown that drift-collection calorimeters can deliver high quality calorimetry at low cost. The long drifting in thin gaps that is needed is shown to be practical using resistive ink and focussing drift fields. Electrodeless chambers offer the possibility of simplified construction and perhaps compensation for curved geometries and magnetic fields. A particular calorimeter design for use at SLC is presented.

Table I. Suggested Parameters for SLC Calorimeter

		ELECTROMAGNETIC	HADRONIC
Plate thickness		0.2 X_0	0.2 Λ_i
Drift gap		3 mm	6 mm
Drift distance		30 cm	40-70 cm
Total thickness		15 X_0	5 Λ_i
Polar segmentation (drift)		1.5 mrad	1.5 mrad
Azimuthal segmentation		25 mrad	25 mrad
Longitudinal segmentation		3 segments	3 segments
Channels	Barrel:	7500	7500
	Endcap:	4250	4250
Energy resolution x $\sqrt{E}$		0.12	Fe: 0.60 U: 0.35
Drift Electric Field		200 V/cm	
Drift chamber gas		90% Ar, 10% CO	
Drift velocity		1 cm/μsec	

X_0 = radiation lengths
Λ_i = nuclear interaction lengths

References

1. L.E. Price, Physica Scripta 23, 685 (1981)
L.E. Price and I. Ambats, IEEE Trans. Nuc. Sci. NS-28 506 (1981)
H.G. Fischer and O. Vllaland, IEEE Trans. Nuc. Sci. NS-27, 381 (1980)

2. J. Bartelt, et al., "Soudan 2, A 1000 Ton Tracking Calorimeter for Nucleon Decay," Univ. Minnesota Preprint COO-1764-410 (1981)

3. Manufactured by Microcircuits Co., New Buffalo, Michigan 49117

4. L.E. Price, et al., IEEE Trans. Nuc. Sci. NS-29, (1982)

5. P.W. Warren and J.H. Parker, Jr., Phys. Rev. 128, 2661 (1962)

6. SLC Workshop Report, SLAC (1982)

7. J. Allison, et al., U. Manchester Preprint MC81/33 (1981)

8. Ch. Becker, et al., Siegen Univ. Report SI-82-1, (1982)